Singular value decomposition analyses of tropical tropospheric ozone determined from TOMS

J. H. Kim,[1,2] S. Na,[1] R. V. Martin,[3,4] K. H. Seo,[1] and M. J. Newchurch[2]

Received 29 February 2008; revised 14 May 2008; accepted 27 June 2008; published 14 August 2008.

[1] A controversial dispute in space-based tropospheric ozone remote sensing is the puzzling discrepancy in the spatiotemporal distribution between residual-based satellite ozone observations and biomass-burning activity in the tropics during boreal winter. This study focuses on evaluation and analyses of two tropospheric ozone products determined from Earth Probe TOMS measurements: Convective Cloud Differential measurements (CCD) and Scan Angle measurements (SAM). Rather than using the typical station-to-station inter-comparison with ozone sounding measurements, the evaluation was performed at the global scale using temporal and spatial patterns derived from Singular Value Decomposition (SVD) analyses. The satellite observations of ozone precursors from MOPITT CO and GOME NO_2 serve as markers identifying airmasses influenced by biomass burning. The SVD analyses reveal that the SAM tropospheric ozone product is remarkably consistent (95% significance level) with the two measured ozone precursors, CO and NO_2, in distribution as well as in seasonality. The analyses provide compelling evidence that there is no discrepancy between tropospheric ozone and its precursors during boreal winter. **Citation:** Kim, J. H., S. Na, R. V. Martin, K. H. Seo, and M. J. Newchurch (2008), Singular value decomposition analyses of tropical tropospheric ozone determined from TOMS, *Geophys. Res. Lett.*, *35*, L15816, doi:10.1029/2008GL033690.

1. Introduction

[2] Tropospheric ozone plays a key role in atmospheric oxidation, global warming, and air quality [*Finlayson-Pitts and Pitts*, 1997], which creates a great demand for satellite measurement of tropospheric ozone because of the spatial and temporal coverage available from space-borne observations. The tropospheric ozone residual method (TOR) [*Fishman and Larsen*, 1987; *Hudson and Thompson*, 1998; *Thompson et al.*, 2000; *Valks et al.*, 2003; *Ziemke and Chandra*, 1998] is an indirect determination of tropospheric ozone by subtracting independent estimates of stratospheric ozone from the total atmospheric ozone. One of the striking findings from these TOR methods is the identification of very large amounts of tropospheric ozone from South America across the Atlantic to Africa during austral spring [*Fishman et al.*, 1991]. A series of field campaigns concluded that biomass-burning is a major cause for the widespread ozone pollution. However, none of the residual-based products show a coincident seasonal ozone enhancement over the Northern tropical Atlantic during the Northern tropical biomass-burning season in austral summer and fall that is seen in in-situ [*Martin et al.*, 2002; *Sauvage et al.*, 2007] and satellite Carbon Monoxide (CO) and fire count measurements [*Edwards et al.*, 2003, 2006]. This puzzling discrepancy is known as the "tropical Atlantic paradox" [*Thompson et al.*, 2000].

[3] There have been considerable efforts to resolve the discrepancy. However, although various chemical transport models consider these effects on ozone formation and distribution in their model, simulations of ozone with global tropospheric chemistry models [*Galanter et al.*, 2000; *Hauglustaine et al.*, 1998; *Kim et al.*, 2005; *Lelieveld and Dentener*, 2000; *Martin et al.*, 2002] more closely track the seasonal variation in biomass-burning including enhanced concentrations over Northern Africa during DJF [*Martin et al.*, 2002], than they track the ozone seasonality seen in the residual methods. Direct retrieval of vertically-resolved tropospheric ozone from TES is one of the few products that do not exhibit the discrepancy [*Jourdain et al.*, 2007]. Until now, even though there have been many studies to resolve the discrepancy, none show a satisfactory reconciliation of it.

2. Methodology

[4] Only some satellite-derived tropospheric ozone products exhibit the discrepancy, including all products from the TOR method. In contrast with those residual-based products, the Scan Angle geometry Method (SAM) yields a seasonal variation in tropospheric ozone that is consistent with the seasonal variation in biomass-burning inferred from fire counts by the Along Track Scanning Radiometer (ATSR) satellite instrument, from CO by the Measurements Of Pollution In The Troposphere (MOPITT) satellite instrument, and from global simulations [*Kim et al.*, 2001, 2005]. Tropospheric ozone determined from the Tropospheric Emission Spectrometer (TES) satellite instrument also observed a seasonal variation in tropospheric ozone consistent with biomass-burning [*Beer*, 2006]. However, the optimal estimation method applied to data from the Global Ozone Monitoring Experiment (GOME) satellite instrument also results in the discrepancy [*Liu et al.*, 2006]. Furthermore, the TOR between the Ozone Mapping Instrument (OMI) and MLS stratospheric ozone still indicates the existence of the discrepancy [*Ziemke et al.*, 2006]. The spatial coverage of ozonesonde measurements is

[1]Division of Earth Environmental Systems, Pusan National University, Pusan, Korea.
[2]Atmospheric Science Department, University of Alabama in Huntsville, Huntsville, Alabama, USA.
[3]Department of Physics and Atmospheric Science, Dalhousie University, Halifax, Nova Scotia, Canada.
[4]Harvard-Smithsonian Center for Astrophysics, Cambridge, Massachusetts, USA.

0094-8276/08/2008GL033690$05.00

Table 1. Square Covariance Fraction of the Total Covariance and Coupling Correlation Coefficient Between the Expansion Coefficients of Scan Angle Method Tropospheric Ozone and MOPITT CO, and between Convective-Cloud-Differential Tropospheric Ozone and MCO Corresponding to the Two Leading Singular Value Decomposition Modes

	SCF		r	
Mode	SAMTO-MCO	CCDTO-MCO	SAMTO-MCO	CCDTO-MCO
1	74%	75%	0.97	0.97
2	23%	19%	0.85	0.94

insufficient for evaluation of satellite measurements [*Sun*, 2003]. Our approach is to examine the existence of the discrepancy by comparing the two kinds of products with satellite observations of biomass burning, which is expected to efficiently produce ozone in the tropics [*Crutzen and Andreae*, 1990; *Lelieveld et al.*, 2004]. A promising statistical tool for identifying these coupled relationships with spatial-temporal pattern between two data sets is analysis with Singular Value Decomposition (SVD) [*Venegas et al.*, 1997; *Yun and Kwon*, 2002]. This method is applied to two variables (e.g., O_3 and CO) in order to detect temporally synchronous and coupled spatial patterns between the two variables. This detection is accomplished by finding linear combinations of the two variables such that the linear combinations retain maximum possible covariance. In other words, the SVD provides a useful tool to diagnose the spatial and temporal coherence of two fields in a global perspective. These coherences serve to identify parsimoniously the times and locations of phenomena that make physical sense (see auxiliary material for more detail[1]).

[5] Four kinds of satellite data products have been used in this study: MOPITT CO (MCO) from the Terra satellite (http://web.eos.ucar.edu), GOME NO_2 ($GOMENO_2$) from GOME (http://www.temis.nl), SAM-tropospheric ozone (SAMTO; http://www.nsstc.uah.edu/atmchem), and convective-cloud-differential (CCD)-method-tropospheric ozone (CCDTO; http://toms.gsfc.nasa.gov), which is the most widely used residual-based product; both SAM and CCD are derived from Earth Probe TOMS. Monthly averages are calculated for all four data products over the Earth Probe TOMS period between August 1996 and December 2000. The area of interest for our study is in the tropics between 15° South and 15° North.

3. Results and Discussion

[6] SVD of the cross-covariance matrix between two fields such as SAMTO and MCO, CCDTO and MCO, SAMTO and $GOMENO_2$, or CCDTO and $GOMENO_2$ identifies modes of behavior in which the satellite ozone and CO (or NO_2) variations are strongly coupled. Table 1 displays the fraction variance (labeled Square Covariance Fraction, SCF, after *Venegas et al.* [1997]) explained by each mode and also the correlation coefficient, r, between expansion coefficients of the SAMTO and MCO, and CCDTO and MCO, as indicators of the strength of the coupling. The SVD squared singular values (analogous to the eigenvalues of univariate analysis) represent the covariance captured by that singular vector (analogous to eigenvectors). The expansion coefficients are the projection of the singular vectors onto the original data field. See auxiliary material for more details. The first two leading SVD modes (singular vectors) of the coupled SAMTO and MCO account for a squared covariance fraction (SCF) of 97% of the total whose first and second modes are 74% and 23%, respectively. The values are almost the same for the coupled CCDTO and MCO with two leading SVD modes of 75% and 19%, respectively. Because these results show that the first mode exhibits the strongest and most significant coupling between SAMTO and MCO as well as between CCDTO and MCO, this study focuses only on the analyses of the first SVD mode.

[7] Figure 1 shows maps of the expansion coefficients, the coupled spatial patterns (called the heterogeneous correlation map) [*Cherry*, 1996], and also the time series of the expansion coefficients of the first SVD mode of the coupled variables SAMTO and MCO. The dotted region represents the area significant at the 95% confidence level [*Wilks*, 1995]. Figures 1a and 1b depict the spatial patterns of SAMTO and MCO with SCF of 74% and Figure 1c shows the corresponding time series of both SAMTO and MCO. The spatial pattern of MCO in Figure 1a shows a seasonal maximum over the northern equatorial region, especially Northern Africa and Indochina in the February–March period, and over the southern equatorial region, especially South America and Southern Africa in the September–October period. The distribution of fire counts from ATSR (Figure S1) strongly indicates that the spatial pattern of MCO in the first SVD mode is likely due to biomass-burning. The spatial pattern of MCO in Figure 1a is very similar to that of SAMTO in Figure 1b, especially over South America, Africa, and South Asia where biomass-burning signal is apparent. This correspondence suggests that biomass-burning emissions are responsible for most of the coupled statiotemporal variability. Figure 1c shows that the seasonal cycle of both SAMTO and MCO is captured with a correlation coefficient of 0.97. The period for maximum MCO in the Northern equatorial region is February–March; whereas, the period for SAMTO is about a month prior. Similarly, the period of maximum MCO, September–October, in the Southern region occurs one month later than the SAMTO maximum in August–September. Carbon monoxide has a tropical lifetime of several weeks, considerably longer than the ozone lifetime of several days in tropical regions influenced by biomass burning [*Duncan et al.*, 2007; *Jacob et al.*, 1996]. Therefore, a one-month lag between SAMTO and MCO is consistent with the difference in the lifetimes between these two species.

[8] Figures 2a and 2b depict the spatial pattern of CCDTO and MCO with an SCF of 75%. Strong coherence in the time series is observed between CCDTO and MCO from Figure 2c reflecting the biomass-burning influence. However, the spatial patterns of the two fields are very different from each other throughout the tropics except for the limited regions of South America and southern Africa. This result is consistent with the previous finding that the discrepancy is not confined to the Northern Atlantic,

[1] Auxiliary materials are available in the HTML. doi:10.1029/2008GL033690.

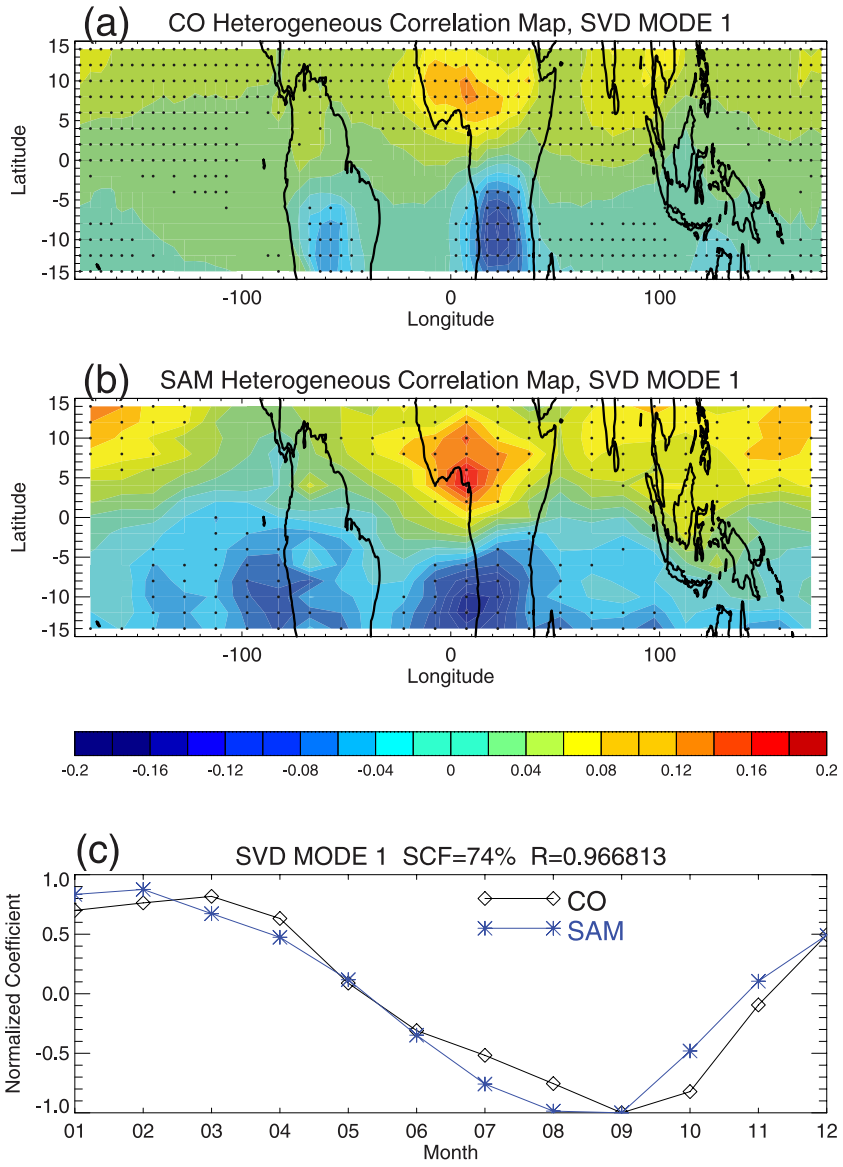

Figure 1. The spatial pattern (heterogeneous correlation map of the first SVD mode for (a) MOPITT CO, (b) SAM tropospheric ozone, and (c) expansion coefficient time series of two variables. Dotted region represents the area significant at the 95% confidence level.

but extends over a broad region of the Northern tropics [*Kim et al.*, 2005; *Martin et al.*, 2002]. Moreover, the covariability between CCDTO and MCO even over South America and southern Africa is shown to be weak and is not statistically significant. Meanwhile, the coherent signal over these regions between SAMTO and MCO is apparent and significant at the 95% confidence level [*Wilks*, 1995].

[9] We assess the statistical robustness of the results obtained from the above SVD analysis, with a significance test using a Monte Carlo approach focusing on the square covariance (SC) rather than the SCF or correlation coefficient [*Venegas et al.*, 1997]. The SC is a direct measure of the relationship between SAMTO and MCO; whereas, the SCF and the correlation coefficient are an indirect measure of the relationship between the coupled SVD patterns.

[10] To perform the Monte Carlo test, we randomized the data by scrambling the 12 monthly means, performing the

Table 2. Square Covariance Fraction and Coupling Correlation Coefficient Between the Expansion Coefficients of SAMTO and GOMENO2 and Between CCDTO and $GOMENO_2$ Corresponding to the Two Leading SVD Modes

	SCF		r	
Mode	$SAMTO\text{-}GOMENO_2$	$CCDTO\text{-}GOMENO_2$	$SAMTO\text{-}GOMENO_2$	$CCDTO\text{-}GOMENO_2$
1	87%	76%	0.98	0.89
2	11%	19%	0.19	0.90

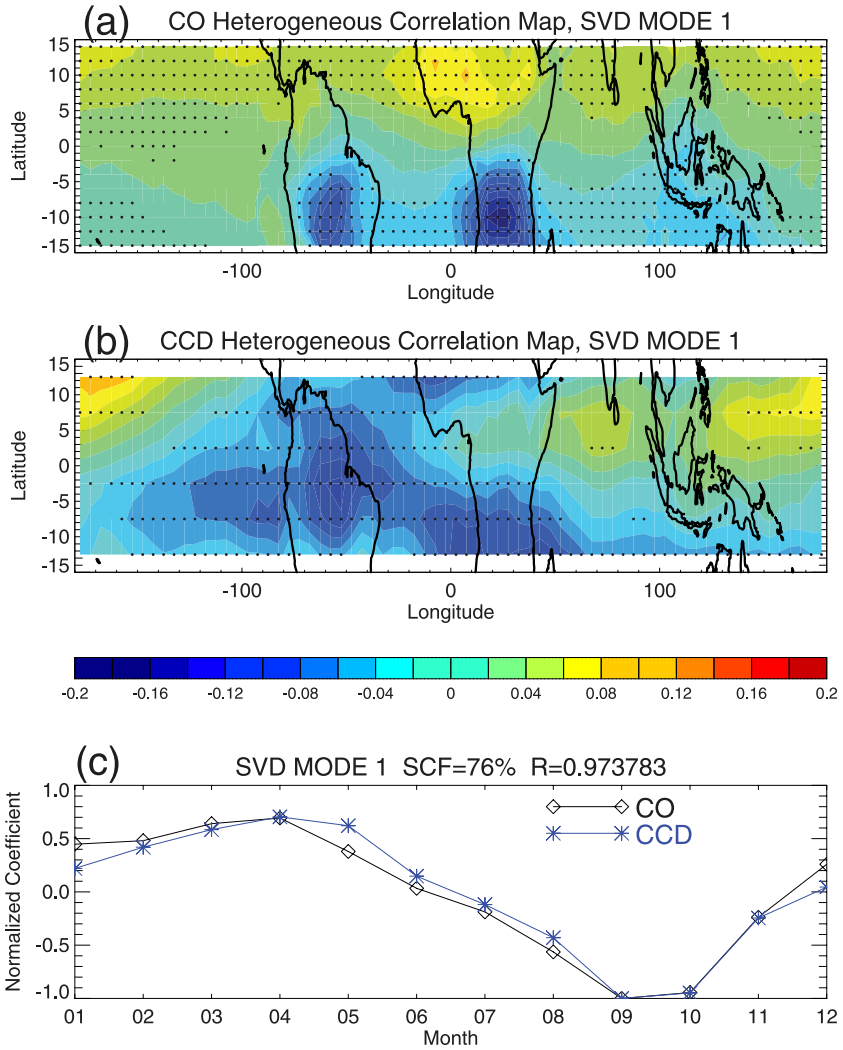

Figure 2. The spatial pattern (heterogeneous correlation map of the first SVD mode for (a) MOPITT CO, (b) CCD tropospheric ozone, and (c) expansion coefficient time series of two variables. Dotted region represents the area significant at the 95% confidence level.

SVD analysis on the scrambled datasets, and repeating the same procedure 500 times. An SC value from the original datasets is statistically significant at the 95% level [(1−7/500)*100 = 98.6%, which we report, conservatively, as 95%] if it is not exceeded by more than five values of the corresponding SC from the random datasets [*Venegas et al.*, 1997]. The results of the 500 scrambled SVD analyses appear in Figure S2, together with the results of the original SVD. The observed SC of the first mode is highly significant at greater than the 95% level, confirming that the spatiotemporal pattern between SAMTO and MCO is extremely robust.

[11] Similar SVD random-test analyses between SAMTO and $GOMENO_2$ as well as CCDTO and $GOMENO_2$ produce Table 2 results of the SCF and correlation coefficient of two coupled fields: SAMTO and $GOMENO_2$; CCDTO and $GOMENO_2$. The first SVD mode of coupled SAMTO and $GOMENO_2$ accounts for SCF of 87% of TSC. The first SVD mode of coupled CCDTO and $GOMENO_2$ accounts for 76%.

[12] Figure 3 shows the coupled spatial and temporal pattern of the first SVD mode between SAMTO and $GOMENO_2$. Figures 3a and 3b depict the spatial pattern of SAMTO and $GOMENO_2$ with SCF of 87%. Here, we focus on only the first SVD mode for this coupled field because of its significance. The north−south gradient of the $GOMENO_2$ spatial pattern over the Pacific Ocean is not as significant as that of SAMTO in Figure 3c. Nonetheless, based on the coincidence in spatial pattern and time series between ATSR fire counts (Figure S1) and Figure 3, the spatial pattern of $GOMENO_2$ in the first SVD mode occurs likely due to biomass burning. The time series of ozone in Figure 3c coincides with NO_2, where about a month lag occurs in the time series between ozone and CO. The lifetime of NO_x ($NO+NO_2$) [*Jaeglé et al.*, 1998; *Wenig et al.*, 2003] is typically within several days of the ozone lifetime in regions influenced by biomass burning, supporting the coherence in time series of ozone and NO_2 in Figure 3c. Using the Monte Carlo test, the observed SC of the first mode is highly significant at greater than the 95% level; and thereby, the coherence between SAMTO and $GOMENO_2$ is robust.

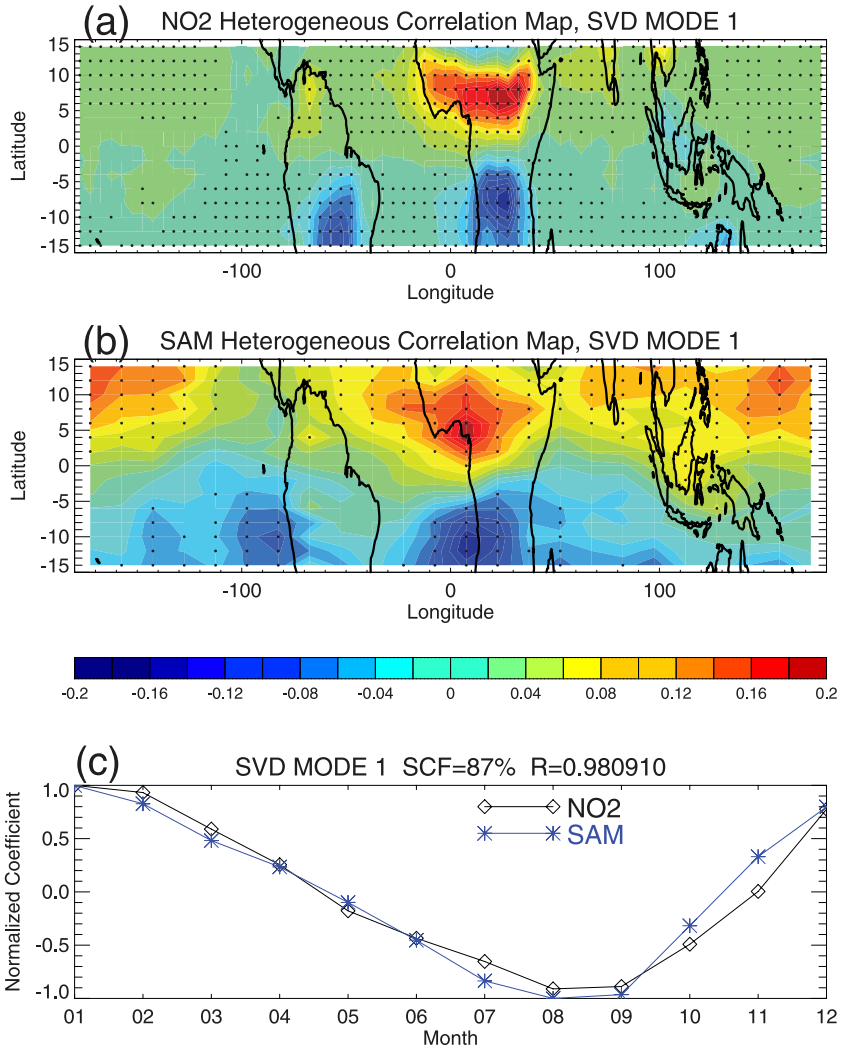

Figure 3. The spatial pattern (heterogeneous correlation map of the first SVD mode for (a) GOME NO_2, (b) SAM tropospheric ozone, and (c) expansion coefficient time series of two variables. Dotted region represents the area significant at the 95% confidence level.

[13] The spatial and temporal pattern of the first SVD mode between CCDTO and GOMENO_2 appears in Figure S3. As with the pattern between CCDTO and MCO in Figure 2, little coherence exists between CCDTO and GOMENO_2 in the northern tropics.

4. Conclusion

[14] This study focused on evaluation and analyses of two tropospheric ozone products determined from Earth Probe TOMS measurements: CCD and SAM. Instead of using the typical station-to-station inter-comparison with ozonesounding measurements, the evaluation adopted a global perspective of temporal and spatial patterns derived from Singular Value Decomposition (SVD) analyses. The ozone precursors, which are CO from MOPITT and NO_2 from GOME, serve as markers of identifying airmasses influenced by biomass burning.

[15] The SVD analyses provide conclusive evidence that the SAM tropospheric ozone product is remarkably consistent with the two measured ozone precursors, CO and NO_2, observed from MOPITT and GOME sensors, in distribution as well as in seasonality and is consistent with chemical theory and in-situ measurements [*Martin et al.*, 2002; *Moxim and Levy*, 2000; *Sauvage et al.*, 2007]. TES retrievals of tropospheric ozone also indicate a seasonal enhancement in tropospheric ozone over the northern tropical Atlantic that supports our conclusions [*Jourdain et al.*, 2007]. The residual-based ozone products, however, are not consistent with the spatial distribution of a major ozone source, biomass burning, and its temporal variation. The Monte Carlo test demonstrates that the evidence from the SVD analyses is statistically robust. The agreement in the first SVD mode between SAM tropospheric ozone and MOPITT CO as well as GOME NO_2 suggests that biomass-burning is an important driving mechanism for tropospheric ozone production in the northern tropics. These analyses provide compelling evidence that there is no discrepancy between tropospheric ozone and its precursors during boreal winter.

[16] **Acknowledgments.** This work was supported by NASA and Ministry of Environment as the Korea Eco-technopia 21.

References

Beer, R. (2006), AURA TES: 2 Years on Orbit, *Eos Trans. AGU*, *87*(52), Fall Meet. Suppl., Abstract A42A-02.

Cherry, S. (1996), Singular value decomposition analysis and canonical correlation analysis, *J. Clim.*, *9*(9), 2003–2009.

Crutzen, P. J., and M. D. Andreae (1990), Biomass burning in the tropics: Impact on atmospheric chemistry and biogeochemical cycles, *Science*, *250*(4988), 1669–1679.

Duncan, B. N., J. A. Logan, I. Bey, I. A. Megretskaia, R. M. Yantosca, P. C. Novelli, N. B. Jones, and C. P. Rinsland (2007), Global budget of CO, 1988–1997: Source estimates and validation with a global model, *J. Geophys. Res.*, *112*, D22301, doi:10.1029/2007JD008459.

Edwards, D. P., et al. (2003), Tropospheric ozone over the tropical Atlantic: A satellite perspective, *J. Geophys. Res.*, *108*(D8), 4237, doi:10.1029/2002JD002927.

Edwards, D. P., et al. (2006), Satellite-observed pollution from Southern Hemisphere biomass burning, *J. Geophys. Res.*, *111*, D14312, doi:10.1029/2005JD006655.

Finlayson-Pitts, B. J., and J. N. Pitts Jr. (1997), Tropospheric air pollution: Ozone, airborne toxics, polycyclic aromatic hydrocarbons, and particles, *Science*, *276*(5315), 1045–1052.

Fishman, J., and J. C. Larsen (1987), Distribution of total ozone and stratospheric ozone in the tropics: Implications for the distribution of tropospheric ozone, *J. Geophys. Res.*, *92*(D6), 6627–6634.

Fishman, J., et al. (1991), Identification of widespread pollution in the Southern Hemisphere deduced from satellite analyses, *Science*, *252*(5013), 1693–1696.

Galanter, M., H. Levy II, and G. R. Carmichael (2000), Impacts of biomass burning on tropospheric CO, NO_x, and O_3, *J. Geophys. Res.*, *105*(D5), 6633–6653.

Hauglustaine, D. A., G. R. Brasseur, S. Walters, P. J. Rasch, J.-F. Müller, L. K. Emmons, and M. A. Carroll (1998), MOZART, a global chemical transport model for ozone and related chemical tracers: 2. Model results and evaluation, *J. Geophys. Res.*, *103*(D21), 28,291–28,335.

Hudson, R. D., and A. M. Thompson (1998), Tropical tropospheric ozone from Total Ozone Mapping Spectrometer by a modified residual method, *J. Geophys. Res.*, *103*(D17), 22,129–22,145.

Jacob, D. J., et al. (1996), Origin of ozone and NO_x in the tropical troposphere: A photochemical analysis of aircraft observations over the South Atlantic basin, *J. Geophys. Res.*, *101*(D19), 24,235–24,250.

Jaeglé, L., D. J. Jacob, Y. Wang, A. J. Weinheimer, B. A. Ridley, T. L. Campos, G. W. Sachse, and D. E. Hagen (1998), Sources and chemistry of NO_x in the upper troposphere over the United States, *Geophys. Res. Lett.*, *25*(10), 1705–1708.

Jourdain, L., et al. (2007), Tropospheric vertical distribution of tropical Atlantic ozone observed by TES during the northern African biomass burning season, *Geophys. Res. Lett.*, *34*, L04810, doi:10.1029/2006GL028284.

Kim, J. H., et al. (2001), Distribution of tropical tropospheric ozone determined by the scan-angle method applied to TOMS measurements, *J. Atmos. Sci.*, *58*(18), 2699–2708.

Kim, J. H., S. Na, M. J. Newchurch, and R. V. Martin (2005), Tropical tropospheric ozone morphology and seasonality seen in satellite and in situ measurements and model calculations, *J. Geophys. Res.*, *110*, D02303, doi:10.1029/2003JD004332.

Lelieveld, J., and F. J. Dentener (2000), What controls tropospheric ozone?, *J. Geophys. Res.*, *105*(D3), 3531–3551.

Lelieveld, J., et al. (2004), Increasing ozone over the Atlantic Ocean, *Science*, *304*(5676), 1483–1487.

Liu, X., et al. (2006), First directly retrieved global distribution of tropospheric column ozone from GOME: Comparison with the GEOS-CHEM model, *J. Geophys. Res.*, *111*, D02308, doi:10.1029/2005JD006564.

Martin, R. V., et al. (2002), Interpretation of TOMS observations of tropical tropospheric ozone with a global model and in situ observations, *J. Geophys. Res.*, *107*(D18), 4351, doi:10.1029/2001JD001480.

Moxim, W. J., and H. Levy II (2000), A model analysis of the tropical South Atlantic Ocean tropospheric ozone maximum: The interaction of transport and chemistry, *J. Geophys. Res.*, *105*(D13), 17,393–17,415.

Sauvage, B., et al. (2007), Remote sensed and in situ constraints on processes affecting tropical tropospheric ozone, *Atmos. Chem. Phys.*, *7*(3), 815–838.

Sun, D. (2003), Tropical tropospheric ozone: New methods, comparisons, and model evaluations of controlling processes, Ph.D. dissertation, Univ. of Ala., Tuscaloosa.

Thompson, A. M., B. G. Doddridge, J. C. Witte, R. D. Hudson, W. T. Luke, J. E. Johnson, B. J. Johnson, S. J. Oltmans, and R. Weller (2000), A tropical Atlantic paradox: Shipboard and satellite views of a tropospheric ozone maximum and wave-one in January–February 1999, *Geophys. Res. Lett.*, *27*(20), 3317–3320.

Valks, P. J. M., R. B. A. Koelemeijer, M. van Weele, P. van Velthoven, J. P. F. Fortuin, and H. Kelder (2003), Variability in tropical tropospheric ozone: Analysis with Global Ozone Monitoring Experiment observations and a global model, *J. Geophys. Res.*, *108*(D11), 4328, doi:10.1029/2002JD002894.

Venegas, S. A., et al. (1997), Atmosphere-ocean coupled variability in the South Atlantic, *J. Clim.*, *10*, 2904–2920.

Wenig, M., et al. (2003), Intercontinental transport of nitrogen oxide pollution plumes, *Atmos. Chem. Phys.*, *3*(2), 387–393.

Wilks, D. S. (1995), *Statistical Methods in the Atmospheric Sciences*, Int. Geophys. Ser., vol. 59, 467 pp., Academic, San Diego, Calif.

Yun, W. T., and W. T. Kwon (2002), SVP multi-model superensemble technique for long-term prediction, *Korean J. Atmos. Sci.*, *5*, 217–228.

Ziemke, J. R., and S. Chandra (1998), Comment on "Tropospheric ozone derived from TOMS/SBUV measurements during TRACE A" by J. Fishman et al., *J. Geophys. Res.*, *103*(D12), 13,903–13,906.

Ziemke, J. R., S. Chandra, B. N. Duncan, L. Froidevaux, P. K. Bhartia, P. F. Levelt, and J. W. Waters (2006), Tropospheric ozone determined from Aura OMI and MLS: Evaluation of measurements and comparison with the Global Modeling Initiative's Chemical Transport Model, *J. Geophys. Res.*, *111*, D19303, doi:10.1029/2006JD007089.

J. H. Kim, S. Na, and K. H. Seo, Division of Earth Environmental Systems, Pusan National University, Pusan, 609-735, Korea.

R. V. Martin, Department of Physics and Atmospheric Science, Dalhousie University, Halifax, NS B3H 3J5, Canada.

M. J. Newchurch, Atmospheric Science Department, University of Alabama in Huntsville, 320 Sparkman Drive, Huntsville, AL 35805, USA. (mike@nsstc.uah.edu)